Abstract

This work analyses the performance of diversity receivers and M-ary modulation over hoyt fading channels. M-ary modulation scheme has been tested on hoyt fading channel as it is more realistic representation of fading in satellite link. We have tested it for 16-PSk, 4-PSK and 32 PSK scheme for various fading and correlation coefficient parameters of hoyt channel. Hoyt channel is derived form nakagami-m channel and also known as nakagami-q channel. The classical PDF based approach has been followed to derive the performance measures of basic diversity combiners namely Maximal ratio combining (MRC) receiver over Hoyt. The analysis is carried out for both independent and correlated fading channels for various coherent and noncoherent modulation schemes. For independent diversity receivers the analysis has been carried out for arbitrary number of input branches. The effect of diversity order and fading parameters on performance measures is studied with the help of the numerical evaluation of the obtained expressions. For dual correlated receivers the analysis is carried out for arbitrary correlation, whereas for L diversity receivers it is for most important practical correlation models exponential correlation. Exponential correlation is used to model the system when the receiving antennas are placed in a linear array. The effect of correlation on the receiver performance is studied for all the systems. To validate the derived expressions Monte carlo simulation is performed.

CHAPTER 1

INTRODUCTION

In past few years, wireless communication has played an important role in information technology as information can be transmitted without the need of dedicated link between transmitter and receiver unlike wired communication, where a dedicated link/channel exist between transmitter and receiver. Compared to wired communication systems, wireless systems introduce a very interesting feature ‘mobility’. In any kind of communication, wired or wireless, there are some parameters like bandwidth, transmitted power, data rate etc. which decide the reliability of a system. The one which optimizes all of them is said to be a perfect system. In recent years, lots of research has been done on both kinds of communication so that a reliable system can be designed with high bandwidth, low transmitted power, high data rates and low bit or symbol error probability.

1.1 Wireless Communication System

In a wireless communication system, data is transmitted in the form of electromagnetic waves using antennas. When signal propagates through the wireless media, phenomena such as reflection and scattering through buildings, trees etc. and refraction through the edges causes the signal to follow multiple paths having different path loss factors and different delays. Thus, at the receiver, the received signal consists of multiple copies of same information bearing signal having different amplitudes and different phases arising due to different path lengths. Figure 1.1 shows a typical urban/suburban mobile radio environment. In the figure

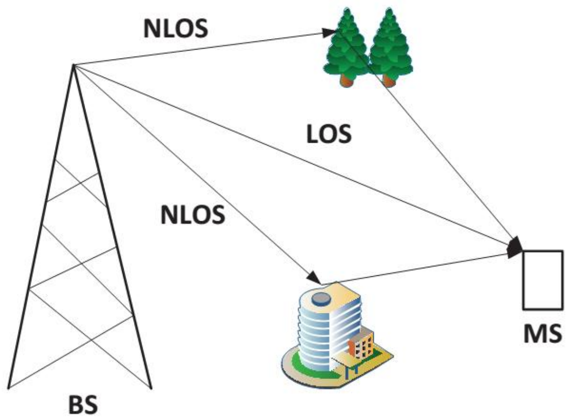

Figure 1.1: A typical urban/suburban mobile radio environment [1]

the direct path between the transmitter and the receiver is called line-of-sight (LOS) path, whereas, the path corresponding to reflected signal is called non line-of-sight (NLOS) path. These multipaths have different phases corresponding to different path-delays, so that they interfere at the receiver either constructively or destructively resulting in variation in signal-to-noise ratio. In addition, mobility introduces time variation in channel response, i.e. if a very short pulse is transmitted, the received signal appears as a train of pulses due to presence of multipaths. Secondly, as a result of time varying response, if same procedure is followed multiple times, a change is observed in the received pulse train over time, which will include changes in the sizes of individual pulses, changes in relative delays among the pulses and often, changes in the number of pulses observed. Hence, the equivalent low-pass time varying impulse response of the channel can be modeled as [1]:

$$c(\tau; t) = \sum_i \alpha_i(t) e^{-j2\pi f_c \tau_i(t)} \delta[t - \tau_i(t)] \tag{1.1}$$

where, $\alpha_i(t)$ and $\tau_i(t)$ are time varying attenuation factor and path delay for ith path respectively. For a transmitted signal s(t) = 1 the received signal for the case of discrete multipath is given by [1]:

$$r_l(t) = \sum_i \alpha_i(t) e^{-j\theta_i(t)}$$

The $\alpha_i(t)$ and $\tau_i(t)$ associated with different signals vary at different rates and in random manner. So, received signal $r_l(t)$ can be modelled as a random process. For large number of paths, central limit theorem can be applied and $r_l(t)$ can be modeled as complex-valued Gaussian random process i.e. c(τ ;t) is also a complex-valued random process in t variable [1].

1.1.1 Fading

Due to time varying nature of phases and amplitudes of the received signals, the multipaths add constructively or destructively at the receiver resulting in fluctuation in the received signal. This amplitude variations in the received signal is termed as fading. There are some parameters which define the fading characteristics of the channel. These parameters are:

Coherence Time

Coherence time, Tc of the channel measures the period of time over which two samples of channel response taken at same frequency but at different time instants are correlated. The coherence time is also related to Doppler spread, fd by [1]:

$$T_c \cong \frac{1}{f_d}$$

Coherence Bandwidth

Coherence bandwidth, fc of the channel measures the frequency range over which two samples of channel response taken at same time instants but at different frequencies are correlated. The coherence bandwidth is related to maximum delay spread, τmax by [1]:

$$f_c \cong \frac{1}{\tau_{max}}$$

Depending upon the parameters described above, fading can be classified into four groups:

1.1.1.1 Slow and Fast Fading

In slow fading, the symbol time duration Ts is smaller than the channel's coherence time, so that multiple symbols undergo same fading. Whereas, in fast fading, the symbol time duration Ts is larger than the channel's coherence time, hence, fading decorrelates from symbol to symbol [2].

1.1.1.2 Frequency-Flat and Frequency-Selective Fading

Fading is said to be frequency-flat, if signal bandwidth is less than channel's coherence bandwidth fc, i.e. all spectral components of the signal undergo same fading. In frequency-selective fading, signal bandwidth is greater than channel's coherence bandwidth, so different spectral components of the signal are affected by different fading [2]. Frequency selectivity results in inter-symbol interference (ISI).

1.1.2 Statistical Models for Fading Channels

As wireless channel impulse response is modeled as a random process, multiple distributions have been developed to model the fading channel. For large number of scatterers, central limit theorem can be applied and channel response c(τ ;t) can be modeled as a complex-valued Gaussian random process. When the impulse response c(τ ;t) is modeled as zero-mean complex random process, the envelope |c(τ ;t)| is Rayleigh distributed and phase ∠c(τ ;t) is uniformly distributed. If there are fixed scatterers in addition to randomly moving scatterers, c(τ ;t) can be modeled as non-zero mean complex Gaussian process so that envelope |c(τ ;t)| is Rice distributed [1]. Different fading models are described below.

1.1.2.1 Rayleigh Model

Rayleigh model is used when there is no LOS component present in the received signal. The probability density function (PDF) of the envelope α ≥ 0 of channel impulse response is given as [2]:

$$p_\alpha(\alpha) = \frac{2\alpha}{\Omega} e^{\frac{-\alpha^2}{\Omega}} \qquad \alpha \geq 0$$

1.1.2.2 Nakagami-n (Rice) Model

Nakagami-n distribution is also called Rice distribution. This is suitable for the propagation paths having one strong LOS path and many weaker NLOS paths. The pdf is given as [2]:

$$p_\alpha(\alpha) = \frac{2(1+n^2)e^{-n^2}\alpha}{\Omega} e^{\frac{-(1+n^2)\alpha^2}{\Omega}} I_o(2n\alpha\sqrt{\frac{1+n^2}{\Omega}}) \qquad \alpha \geq 0$$

where, 0 ≤ n ≤ ∞ is the Nakagami-n fading parameter and is related to Ricean factor 'K' by K=n 2 . I0(·) is bessel's function of first kind and order zero [3]. Nakagami-n distribution includes the Rayleigh distribution as a special case (n=0) and spans from Rayleigh fading (n=0) to no-fading (n=∞).

1.1.2.3 Nakagami-q Model

The PDF of Nakagami-q distributed RV is given as [2]:

$$p_\alpha(\alpha) = \frac{2(1+q^2)\alpha}{\mathrm{q}\Omega} e^{\frac{-(1+q^2)\alpha^2}{4q^2\Omega}} I_o(2n\alpha\sqrt{\frac{(1-q^2)\alpha^2}{4q^2\Omega}}) \qquad \alpha \geq 0$$

where, 0 ≤ q ≤ 1 is Nakagami-q fading parameter. This fading distribution includes one-sided Gaussian (q=0) and Rayleigh (q=1) as special cases.

1.1.2.4 Nakagami-m Model

The PDF of Nakagami-m distributed random variable (RV) is given as [2]: pα(α) = 2mmα

$$p_\alpha(\alpha) = \frac{2m^m \alpha^{2m-1}}{\Omega^{\mathrm{m}} \tau(\mathrm{m})} e^{\frac{-m\alpha^2}{\Omega}} \qquad \alpha \geq 0$$

where, $\Gamma(\cdot)$ is gamma function [3] and $1/2 \leq m \leq \infty$ is Nakagami-m fading parameter. This fading model includes one-sided Gaussian (m=1/2), Rayleigh (m=1) fading and no-fading (m=∞) as special cases. For m < 1, it closely approximates Hoyt distribution, and this mapping is given by [2]:

$$m = \frac{(1+q^2)^2}{2(1+2q^4)} \qquad m \leq 1$$

Similarly, for m > 1, it closely approximates the Nakagami-n (Rice) distribution and this mapping is one-to-one and given by [2]:

$$m = \frac{(1+n^2)^2}{(1+2n^2)} \qquad 0 \leq n$$

1.2 Effect of Fading on System Performance

Fading, in wireless communication systems, results in poor BER performance as compared to non-fading environment in presence of additive white Gaussian noise (AWGN). This performance degradation arises due to amplitude variation of the received signal because of fading. Figure 1.2 shows the BER curves for Rayleigh faded wireless channel and non-fading AWGN channel over BPSK modulation scheme.

From the figure it can be observed that, to have an BER of 10−3 , SNR needed for non-fading channel is ≃ 7dB, where as for Rayleigh faded channel, it is ≃ 23dB. In such case, the transmitted power for Rayleigh faded channel will be ≈ 40 times that of AWGN channel. To mitigate the effects of fading on the system and to improve performance of the system, Diversity techniques are used at the receiver end.

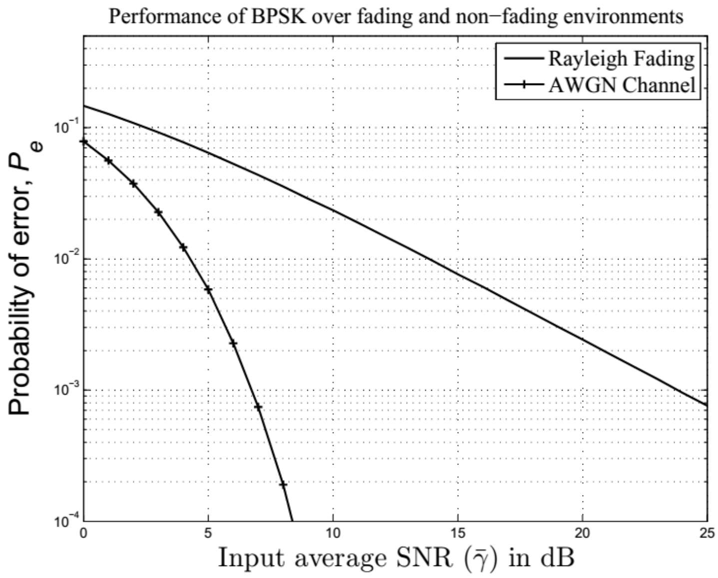

Figure 1.2: Comparison between Rayleigh faded and AWGN Channel

1.2 Diversity

In a typical mobile radio environment, it is observed that if two or more radio channels are sufficiently separated in frequency, time or space, then the fading in various channels is more or less independent. Diversity, is the key technology that uses this independence of channels to mitigate the effect of fading [4]. The main object of diversity techniques is to use several replicas of transmitted signal to improve system performance. There are various ways to obtain independently faded channels:

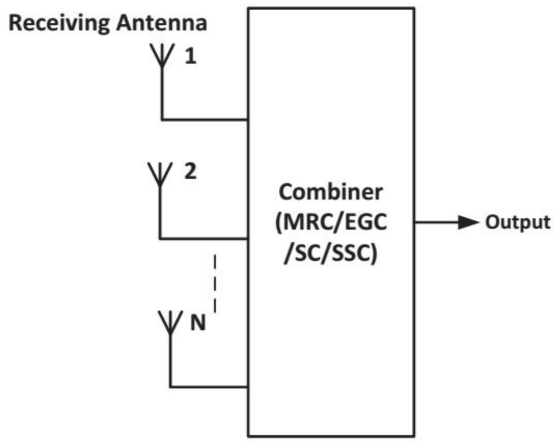

Figure 1.3: Block diagram of Space diversity combiner [4]

• Frequency Diversity: The message is simultaneously transmitted over different carrier frequencies such that the separation between frequencies should be larger than channel's coherence bandwidth.

• Time Diversity: Same message is transmitted over different time slots such that the time separation between adjacent transmissions should be greater than channel's coherence time.

• Space Diversity: Desired message is transmitted/received through multiple transmit/receive antennas separated by at least half of the carrier wavelength. In the case of shadowing, the separation should be at least 10 carrier wavelength.

• Angle Diversity: The message is received simultaneously using multiple antennas pointing in different directions.

The multiple replicas of the transmitted signal obtained using any of the method mentioned above, is then combined efficiently to improve the SNR at the detector input. Figure 1.4 shows a space diversity technique with a combiner, which combines the multiple signals received on different antennas. There are different types of diversity combining techniques, which are discussed in next section:

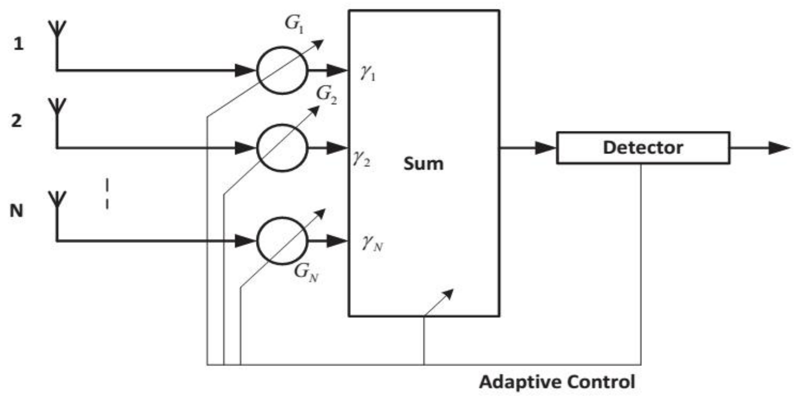

Figure 1.4: Block diagram of Maximal Ratio Combiner [4]

1.3.1 Diversity Combining Techniques

There are different types of diversity combining techniques used in practice [2], which are as follows:

1.3.1.1 Maximal Ratio Combining

In maximal ratio combining technique, the received multiple faded copies of the transmitted signal are co-phased. The co-phased signal copies are weighted individually in proportion to their strength to maximize SNR at the output of the combiner. Assuming the received signal SNR at the input of the combiner is γi , i = 1, 2, ..N, the output SNR can be shown to be [5]:

$$\gamma_{MRC} = \sum_{i=1}^{N} \gamma_i$$

The MRC operation requires estimation of phase and amplitude of each received input branch signal. Hence, the complexity of implementation is high.

1.3.1.2 Equal Gain Combining

Different weights for each branch may not be convenient as it may increase the complexity of the receiver as in the case of MRC. So it is convenient to set all the gains to unity, while cophasing all signals before combining [2]. This technique of combining is called Equal Gain Combining.

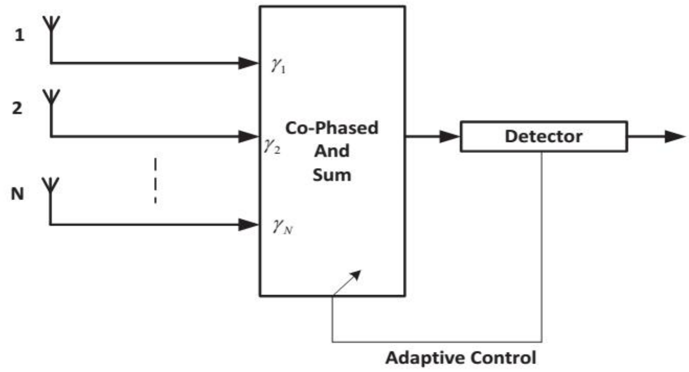

Figure 1.5: Block diagram of Equal Gain Combiner [2]

For EGC, the output SNR is given as [2]:

$$\gamma_{EGC} = \frac{(\sum_{i=0}^{N} \alpha_i^2) E_S}{\sum_{i=0}^{N} P_{N_i}}$$

where, αi is the fading amplitude for ith copy of the transmitted signal.

1.3.1.3 Selection Combining

In selection combining (SC), the system chooses the received signal having maximum SNR out of all copies of signals received. In this scheme the output SNR can be given as [2]:

$$\gamma SC = \max\{\gamma 1, \gamma 2, ..., \gamma N\}$$

1.3.1.4 Switch and Stay Combining

The switch and stay combining (SSC) technique discussed here is presented in [2] and also shown in Figure 1.7. In this system, there are only two copies of fading signals are used. The combiner has only two antennas to receive fading signals. The received signal is fed as shown in Figure 1.7. In this scheme the received SNR $\gamma 1$ at antenna L1 is compared with a predefined threshold γT . Switching occurs to the input branch L2 if $\gamma 1 < \gamma T$. And it again switches to first branch if $\gamma 1 > \gamma T$. It may happen that after switching the input SNR $\gamma 2$ at L2 is less than γT or even less than $\gamma 1$, in such case the switch will still be connected to L2 until the SNR of first branch becomes greater than γT . Switching from branch L2 to branch L1 is done in similar manner.

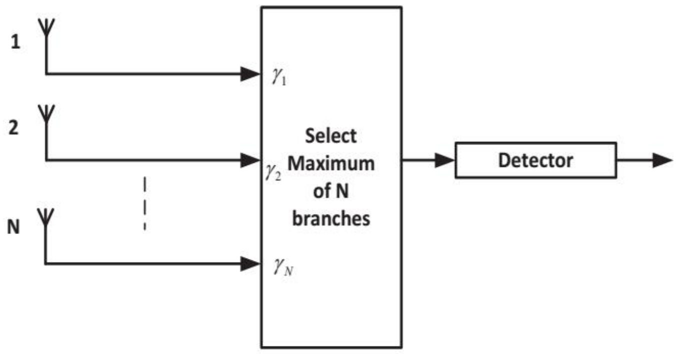

Figure 1.6: Block diagram of Selection Combiner

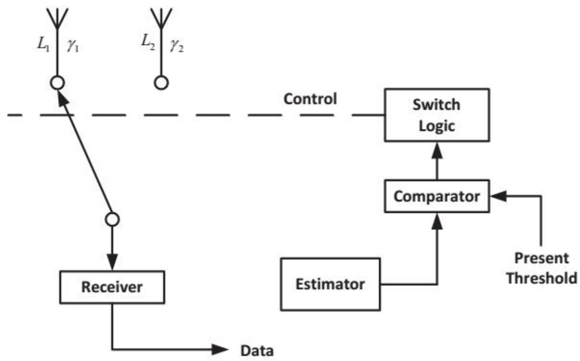

Figure 1.7: Block diagram of Dual branch Switch and Stay Combiner

The SSC output SNR, γSSC can be given as:

$$\gamma_{ssc} = \begin{cases} \gamma_1 & if\ \gamma_1 \geq \gamma_T \\ \gamma_2 & otherwise \end{cases}$$

1.3.1.5 Switch and Examine Combining

Unlike SSC combining scheme, switch and examine combining (SEC) adds the benefit of having multiple branches at the receiver, especially when they are independent and identically distributed (i.i.d.) or equicorrelated and identically distributed. In SSC scheme, receiver switches between the best two paths, adding a path does not improve the performance unless the added path is better than at least one of the best two ones. In SEC combining scheme, the receiver starts examining from the first path. If first path is acceptable, it continues to receiver from it, else, it switches and examines the next available path. This process continues until an acceptable path is found or all paths have been examined. In the latter case, the receiver stays on the last examined path [6] or selects the best path for reception [7].

1.4 Problem Formulation

Performance analysis of digital wireless communications systems usually deals with complicated and cumbersome statistical tasks. One of them arises in the study of diversity combining receivers operating over Hoyt fading channels where the statistics of the sum of squared Hoyt random variables (RVs) (or equivalently the sum of Gamma RVs) are required. Hoyt fading which is observed in satellite links and other fading channels, characterize sever type of fading ranging Gaussian and Rayleigh fading. Well-known applications in the field of satellite systems where such sums could be useful are maximal-ratio combining (MRC) and post-detection equal-gain combining (EGC) or in the evaluation of the outage probability in cellular systems with co-channel interferences. Performance of MRC and EGC over fading channels has been analyzed but these channels were independent fading channels. In practice obtaining independent fading channels for spatial diversity combining is difficult due to size limitations of wireless communication devices. The performance of these independent channels are measured by pdf and cdf for which mathematical formulation is present but if practical dependent fading channel is considered then the solution of these present equations is not sufficient. These equations have to be modified for dependent fading channels which is not done yet efficiently in best of my knowledge.

1.5 **Objective**

As discussed in above chapter, in practice dependent fading channels should be considered, so here in our work we will consider correlated hoyt fading channel and keeping this problem in mind following will be my key objectives:

- To develop a mathematical model of probability distribution function for the MRC (maximal ratio combining) receiver of equally correlated Hoyt fading channel.
- With binary coherent modulation technique, the BER & SNR will be parameters which will analyze the performance of proposed model.
- Proposed model's outcome will be compared with results of Monte Carlo simulation and M-ary modulation techniques also.

CHAPTER 2

LITERATURE REVIEW

In [1] R. Subadar and P. R. Sahu analyzed the performance of an L-MRC receiver in equally correlated Hoyt fading channels and obtain mathematical expressions for the PDF of the MRC output SNR, average SNR and outage probability and ABER expressions for binary, coherent, and non coherent modulations. Numerically evaluated results have been plotted and the impact of fading correlation on the receiver performance is studied. The obtained expressions are in the form of infinite series containing hyper-geometric functions. The numerical results have been compared with available special case results also Monte Carlo simulations outcome are closely matching with numerically obtained results.

In [2] V. Milentijević et.al proposed an approach to the relative measurement error analysis in the process of the Nakagami-m fading signal moments estimation in this paper. Relative error expressions will be also derived for the cases when MRC (Maximal Ratio Combining) diversity technique is performed at the receiver. Capitalizing on them, results will be graphically presented and discussed to show the influence of various parameters, such as diversity order and fading severity on the relative measurement error bounds.

In [3] S. P. Jadhav, V. S. Hendre provided an exact BER analysis for fading channels with maximal-ratio combining (MRC) and imperfect channel estimation at the receive The BER characteristics for the various transmitting and receiving antennas simulated in MATLAB tool box and it shows that the MRC equalizer based receiver is a good choice for removing some ISI and minimizes the total noise power. The results show that the BER decreases as the m x n antenna configurations is increased.

In [4] D.B. Smith and T.D. Abhayapala presented a novel theoretical method to analyse the maximal ratio combining (MRC) receivers using BPSK and M-PSK modulation in spatially correlated Rayleigh fading channels, with perfect and imperfect channel knowledge, in terms of antenna array configuration and parameters of scatterer distributions. In this analysis closed form expressions for error probabilities of these modulations with MRC are derived, allowing for non-distinct eigen values from the channel gain correlation matrix. The results of performance analysis assuming different receiver configurations and scattering scenarios presented give valuable insight into the performance of MRC in practical Rayleigh fading scenarios for isotropic and non-isotropic scatterer distributions.

In [5] R. Subadar analysed the performance of a maximal ratio combining receiver in independent Hoyt fading channels for an arbitrary number (L) of branches. Mathematical expressions for the probability density function of the combiner output signal to-noise ratio, amount of fading, outage probability and the average bit error rate performance for binary, coherent and non-coherent modulations have been presented. A study on the upper bound of the truncation error of the expressions containing infinite series has been provided. Obtained expressions have been numerically evaluated and plotted. A study on the effect of the fading parameter and the number of diversity branches on the receiver performance has also been presented.

In [6] G.K. Karagiannidis et.al presented a unified framework for the error performance of MQAM, employing L-branch equal-gain combining over generalised fading channels, such as Nakagami-m, Rice, Hoyt or Weibull. For each channel model an exact closed-form expression is derived for the moments of the EGC output signal-to-noise ratio (SNR). Using these expressions, the symbol error performance of M-QAM is studied, with the aid of the moment-generating function approach and the Pade approximants theory. The propos! ed mathematical analysis is illustrated by selected numerical results, pointing out the effect of the input SNRs unbalancing, as well as the fading severity on the system's performance. Simulations are also performed to check the validity and the accuracy of the proposed analysis.

In [7] V. G. Venkatesan et al. Presented an exact closed-form expressions for the statistics of the sum of non-identical squared Nakagami-m random variables and it is shown that it can be written as a weighted sum of Erlang distributions. The analysis includes both independent and Nakagami-m cases with distinct average powers and integer-order fading parameters. The proposed formulation significantly improves previously published results which are in the form of infinite sums or higher order derivatives. The obtained formulae can be applied on the performance analysis of maximal-ratio combining diversity receivers operating over Nakagami-m fading channels.

In [8] In - Ho Lee proposed enhanced spatial multiplexing codes (E-SMCs) to enable various encoding rates. Th symbol error rate (SER) performance of the E-SMC is investigated when zero-forcing (ZF) and maximal-ratio combining (MRC) techniques are used at a receiver. The proposed E-SMC allows a transmitted symbol to be repeated over time to achieve further diversity gain at the cost of the encoding rate. With the spatial correlation between transmit antennas, SER equations for M-ary QAM and PSK constellations are derived by using a moment generating function (MGF) approximation of a signal-to-noise ratio (SNR), based on the assumption of independent zero-forced SNRs. Analytic and simulated results are compared for time-varying and spatially correlated Rayleigh fading channels that are modelled as fist-order Markovian channels. Furthermore, we can find an optimal block length for the E-SMC that meets a required SER.

In [9] W. J. L. Queiroz et. al presented a unified analysis for the compact receiver with spatial diversity. The maximum ratio combining (MRC) receiver for linear antenna arrays is considered with the modulation scheme θ-QAM. The mathematical development takes into account parameters related to the physical structure of the array, as well, as the probability distribution used for modeling the direction of arrival (DoA) of the signals in the array. Von Mises and Gaussian distributions are considered to characterize the DoA. The unification of all the results in exact expressions to evaluate the symbol error probability (SEP) at the output of a MRC receiver is the main contribution of the research.

In [10] R.Deepa provided an evaluation of the concept of Spatial Diversity (SD), applied to multi-antenna systems that demand modifications at the physical level - the use of multiple antennas at the transmitter and/or the receiver. The performance of SISO, SIMO, MISO and MIMO systems have been evaluated and compared in AWGN and fading channels.

In [11] A K M Arifuzzman et. al investigated the diversity gain of a Maximal Ratio Combiner (MRC) for Orthogonal Frequency Division Multiplexing (OFDM) by varying the number of receiving antennas. Different modulation schemes namely 64-PSK, 64-QAM, 16-PSK, 16-QAM and QPSK have been used in OFDM technique. The simulation results show that the performance (SNR) of an OFDM system can be significantly improved by using MRC. We have also derived average Symbol Error Rate (SER) of M-ary Quadrature Amplitude (M-QAM) and M-ary Phase Shift Keying (M-PSK) modulations for N-branch MRC space diversity reception scheme. In this paper, it is shown that M-QAM based OFDM technique outperforms M-PSK based OFDM technique. The comparison of the performances of the Signal-to-Noise Ration (SNR) ofM-PSK and M-QAM based OFDM technique has been presented in this paper. It is also shown that SNR can be improved further if the number of receiving antennasis increased.

In [12] V. K. Dwivedi analyzed the performance of OFDM communication system over correlated Nakagami-*m* fading channel using maximal ratio combining (MRC) diversity at the receiver. We have presented new closed form formulas for exact symbol error rate (SER) analysis of the MQAM OFDM communication systems over correlated Nakagami-*m* fading with arbitrary fading index *m*. Using a well known moment generating function (MGF) based analysis, we express the average SER in terms of higher transcendental function such as Appell hyper-geometric function.

In [13] S. Sharma, P. Singh explored the performance analysis of SIMO-OFDM system using different diversity techniques. It has been analyzed that both the powerful techniques MRC and OFDM can perform well when employed with each other, these results are helpful in designing high data rate systems which are working in wireless communication environment with least possible error rate. While in case of presence of number of interferers as it occurs in modern communication channels the OFDM-OC is the best suitable solution for optimal performance.

In [14] S. Chadokar, P. Barmashe analyzed the performance of different diversity techniques, which can be easily applied with orthogonal frequency division multiplexing (OFDM) systems with different equalizing methods. Orthogonal frequency division multiplexing is well known to be a useful technique for high rate data transmission over a frequency selective fading channel. However, for coherent detection of OFDM signals, fading compensation techniques are required to mitigate amplitude and phase distortions due to the multi-path channel fading. The fading compensation technique becomes even more crucial when QAM is used for OFDM systems. A channel estimation technique using periodically inserted pilot symbols in the data stream is well known to provide a reliable way to mitigate the distortions.

In [15] M. Krondorf and G. Fettweis presented a methodology for OFDM link capacity and bit error rate calculation that jointly captures the aggregate effects of various real life receiver imperfections such as: carrier frequency offset, channel estimation error, outdated channel state information due to time selective channel properties and flat receiver I/Q imbalance. Since such an analytical analysis is still missing in literature, we intend to provide a numerical tool for realistic OFDM performance evaluation that takes into account mobile channel characteristics as well as multiple receiver antenna branches. In our main contribution, we derived the probability density function (PDF) of the received frequency domain signal with respect to the mentioned impairments and use this PDF to numerically calculate both bit error rate and OFDM link capacity. Finally, we illustrate which of the mentioned impairments has the most severe impact on OFDM system performance.

In [16] Juan M. Romero-Jerez et. al presented a novel relationship between the distribution of circular and non-circular complex Gaussian random variables. Specifically, we show that the distribution of the squared norm of a non-circular complex Gaussian random variable, usually referred to as squared Hoyt distribution, can be constructed from a conditional exponential distribution. From this fundamental connection we introduce a new approach, the *Hoyt transform* method, that allows to analyze the performance of a wireless link under Hoyt (Nakagami-q) fading in a very simple way. We illustrate that many performance metrics for Hoyt fading can be calculated by leveraging well-known results for Rayleigh fading and only performing a finite-range integral. We use this technique to obtain novel results for some information and communication-theoretic metrics in Hoyt fading channels.

In [17] D. A. Zogas presented an alternative moments-based approach to the performance analysis of equal-gain combining (EGC) receivers over independent, not necessarily identically distributed Riceand Hoyt-fading channels. Exact closed-form expressions for the moments of the signal-to-noise ratio (SNR) at the output of the combiner are derived and significant performance criteria such as, the average output SNR, the amount of fading and the spectral efficiency at the low power regime, are studied. Moreover, using Padé rational approximation to the moment-generating function of the output SNR, the average symbol error probability and the outage probability are evaluated. We also study the suitability of modeling a Hoyt-fading environment by a properly chosen Nakagami- model, as far as the error performance of the EGC is concerned.

In [18]Jos´e F. Paris and David Morales-Jim´enez analysed teh outage probability of Hoyt fading channel. Exact closed-form expressions are obtained for the outage probability of Nakagami-(Hoyt) fading channels under co-channel interference (CCI). The scenario considered in this work assumes the joint presence of background white Gaussian noise and independent Rayleigh interferers with arbitrary powers.

In [19] R. M. Radaydeh analyzed the average bit error rate (BER) of non coherent *M*-ary frequency-shift keying (FSK) signals over multichannel non identically distributed Nakagami- q (Hoyt) fading employing diversity combining. The first part of the paper considers the conventional postdetection non coherent equal-gain combiner (NC-EGC), in which a Fourier series inversion formula is employed to derive a simple and rapidly converging series-based expression for the system average BER. This expression is valid for arbitrary values of received average signal-to-noise ratios (SNRs) and fading parameters. The derived expression is then compared with some existing ones in the literature, and the results show a large reduction in computational complexity, particularly when M and/or the diversity order increases. In the second part, a new non coherent combiner is proposed to achieve improvements over the conventional NC-EGC. It is also shown that this new combiner results in a simple closed-form expression for the system average BER that is given in terms of elementary functions; hence, it can be easily numerically evaluated with noticeable computation efficiency.

In [20] Li Tang Zhu Hongbo simulated and analyzed the statistical perfomances of the Nakagami fading channel in wireless communication with MATLAB, including the complex envelop of received signal, the Level Crossing Rates and Average Fade Durations on the Maximal-Ratio Combining diversity.

In [21] G. S. Prabhu and P. M. Shankar presented an approach to demonstrate flat fading in communication systems, wherein the basic concepts are reinforced by means of a series of MATLAB simulations. Following a brief introduction to fading in general, models for flat fading are developed and simulated using MATLAB. The concept of outage is also demonstrated using MATLAB. We suggest that the use of MATLAB exercises will assist the students in gaining a better understanding of the various nuances of flat fading.

In [22] Md. G. Sadeque at. al described the principal characteristics and modelling for different types of fading channels. Different fading model are applicable for different types of environment. In this paper we present probability density function for Rayleigh, Nakagami, Log-normal and Weibull fading model. An effort has been made to illustrate the performance comparison of different types of fading channel in wireless transmission system.

In [23] G. Fraidenraich presented the dual (2×2) MIMO channel capacity over the Hoyt fading channel. The joint eigenvalue distribution of the channel matrix is obtained and it is shown that the effect of the Hoyt parameter b can degrade around 8.5% the channel capacity. For the $t \times r$ case, an asymptotic result is also derived. All the results are validated by numerical Monte Carlo simulations and are in excellent agreement.

In [24] A. Özgür Yılmaz proposed a method by which the outage probability of block fading channels can be evaluated in a straighforward and computationally efficient manner by utilizing the moment generating function of a single block's mutual information. The flexibility of moment generating functions helps obtain outage probabilities in various cases such as wideband noise jamming and multi-access interference. The effect of discrete input alphabets on outage is also investigated and turns out to be vital especially under interference.

In [25] et.al illustrated the performance comparison of the Rayleigh and Rician fading channel models by using MATLAB simulation in terms of source velocity and outage probability. We have developed algorithms for the Rayleigh and Rician fading channels, which computes the envelop and outage probability. The parameters such as source velocity and outage probability play very important role in the performance analysis and design of the digital communication systems over the multipath fading environment.

Chapter 3

Proposed Work

In our work we have tested the hoyt fading channel performance in two different systems. One is M-ary PSK simulation and other is MRC diversity scheme in monte-carlo simulation for correlated hoyt fading channel. The motivation behind MPSK is to increase the bandwidth efficiency of the PSK modulation schemes. In BPSK, a data bit is represented by a symbol. In MPSK, $n = \log_2 M$ data bits are represented by a symbol, thus the bandwidth efficiency is increased to n times. Among all MPSK schemes, QPSK is the most-often-used scheme since it does not suffer from BER degradation while the bandwidth efficiency is increased. Since the description about M-ary PSK modulation scheme is not so important to inherit in this chapter. So we have put that detail in appendix below.

Correlation among received fading signals cannot be avoided due to reasons discussed in [1, 2]. Analysis of diversity receivers for correlated channels is relatively more complicated compared to the independent fading case. In this section, performance of dual -MRC, receivers are analyzed for correlated Hoyt fading channels. For MRC receiver an analysis for unequal fading parameters is also presented in addition to the equal fading parameter case. Unequal channel fading parameters may be observed in urban fading environments where diversity channels may have different characteristics. In the analysis presented here the PDF based approach is used. Some conditions are followed for MRC simulation which are:

1. We have N receive antennas and one transmit antenna.

2. The channel is flat fading – In simple terms, it means that the multipath channel has only one tap. So, the convolution operation reduces to a simple multiplication.

3. The channel experienced by each receive antenna is randomly varying in time. For the i^{th} receive antenna, each transmitted symbol gets multiplied by a randomly varying complex number h_i. As the channel under consideration is a hoyt channel, the real and imaginary parts of h_i are Gaussian distributed having mean μ_{h_i} and variance $\sigma_{h_i}^2 = 1/2$.

4. The channel experience by each receive antenna is independent from the channel experienced by other receive antennas.

5. On each receive antenna, the noise η_i has the Gaussian probability density function with

$$p(n) = \frac{1}{\sqrt{2\pi\sigma^2}} e^{\frac{-(n-\mu)^2}{2\sigma^2}}$$

with μ =0 and $\sigma^2 = \frac{N_0}{2}$.

The noise on each receive antenna is independent from the noise on the other receive antennas.

6. At each receive antenna, the channel h_i is known at the receiver.

7. In the presence of channel h_i, the instantaneous bit energy to noise ratio at i^{th} receive antenna is $\frac{|h_i|^2 E_b}{N_o}$. For notational convenience, let us define,

$$\gamma_i = \frac{|h_i|^2 E_b}{N_o}$$

3.2 Maximal Ratio Combining diversity scheme

A signal transmitted at a particular carrier frequency and at a particular instant of time may be received in a multipath null. Diversity reception reduces the probability of occurrence of communication failures (outages) caused by fades by combining several copies of the same message received over different channels. In general, the efficiency of the diversity techniques reduces if the signal fading is correlated at different branches. The most common and efficient diversity scheme is maximal ratio combining (MRC). In Maximum Ratio combining each signal branch is multiplied by a weight factor that is proportional to the signal amplitude. That is, branches with strong signal are further amplified, while weak signals are attenuated as shown in figure 3.1.

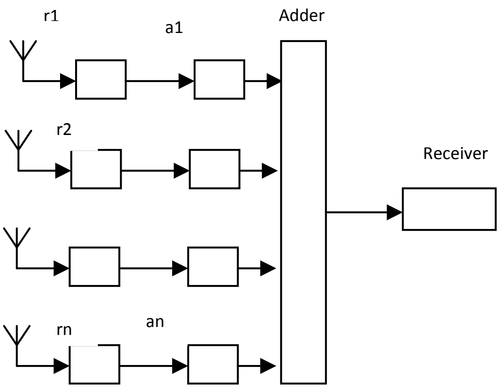

Figure 3.1: L-branch antenna diversity receiver (L = 5). With MRC, the attenuation/amplification factor is proportional to the signal amplitude $a_i = r_i$ for each channel i.

On the i^{th} receive antenna, the received signal is,

$y_i = h_i x + n_i$

Where y_i is the received symbol on the i^{th} receive antenna, h_i is the channel on the i^{th} receive antenna, x is the transmitted symbol and n_i is the noise on i^{th} receive antenna.

y_i Expressing it in matrix form, the received signal is,

Y=hx+n, where

$y = [y_1, y_2, \ldots. y_n]^T$ is the received symbol from all the receive antenna

$h = [h_1, h_2, \ldots. h_n]^T$ is the channel on all the receive antenna

x is the transmitted symbol and

$n = [n_1, n_2, \ldots. n_n]^T$ is the noise on all the receive antenna.

The term, $h^H h = \sum_{i=1}^{N} |h_i|^2$ i.e sum of the channel powers across all the receive antennas.

Complex Gaussian Model of Hoyt Random Variables

The complex Gaussian model of Hoyt RV $\alpha l = |Zl|$ for lth ($l = 1, 2, \ldots, L$) branch can be given as

$Z_l = X_l + jY_l, \qquad l = 1, 2, \ldots, L$

In this representation, the Hoyt RV $\alpha_l = |Z_l|$ has the PDF given in Equation 1.1.2.3. For the convenience of presentation but without loss of generality, we assume $\sigma_{xl} = 1$, this result $\sigma_{yl} = q$. Assuming $\sigma_{xl}^2 = \sigma_x^2$ and $\sigma_{yl}^2 = \sigma_y^2$ $\forall\, l$, from above equation, we can obtain $\Omega_l = E[\alpha_l^2] = 1 + q^2$. Substituting this value of Ωl in Equation 1.1.2.3 and expressing $I0(\cdot)$ in terms of confluent hypergeometric function, Equation 1.1.2.3 can be rewritten as

$$f_{\alpha_l}(\alpha_l) = \frac{\alpha_l e^{-\frac{1}{2q^2}\alpha_l^2}}{q} F_1(\frac{1}{2};1;\frac{1-q^2}{2q^2}\alpha_l^2)$$

For equal branch average power i.e. Ω1 = Ω2 = . . . = ΩL = Ω (equivalently, for $\overline{\gamma_1} = \overline{\gamma_2} = \overline{\gamma_3} \dots \dots .. = \bar{\bar{\gamma}}$), $Eb/N0$ can be expressed in terms of the fading parameter q as

$$\overline{\boldsymbol{\gamma}} = \Omega\left(\frac{Eb}{N0}\right) = (1+q^2)\left(\frac{Eb}{N0}\right)$$

Characteristic Function of Sum of Hoyt Square RVs

In the mathematical model of Hoyt RVs i.e. $\alpha_l^2 = x_l^2 + y_l^2$ is independent. So the joint CF of α2l can be given as

$$\phi_{\alpha_1^2 \dots\dots \alpha_l^2}(j\omega_1, j\omega_1, \dots ., j\omega_L) = \phi_{X_1^2 \dots\dots X_l^2}(j\omega_1, j\omega_1, \dots ., j\omega_L)\phi_{Y_1^2 \dots\dots Y_l^2}(j\omega_1, j\omega_1, \dots ., j\omega_L)$$

An expression for $\phi_{X_1^2 \dots\dots X_l^2}(j\omega_1, j\omega_1, \dots ., j\omega_L)$ can be derived as shown below: From the PDF of Xl, performing transformation of random variable operation, PDF of a Xl2 can be obtained as

$$f_{X_l^2}(X_l^2) = \frac{1}{\sqrt{2\pi\sigma_x^2 x_l}} e^{-\frac{x_l}{2\sigma_x^2}}$$

From above equation X_l^2 can be obtained as

$$\phi_{X_l^2}(j\omega_1) = E\left[e^{j\omega_L x_l}\right] = \frac{1}{(2\pi\sigma_{x^2})^{1/2}} \int_0^\infty \frac{1}{\sqrt{x_l}} e^{-(\frac{1}{2\sigma_{x^2}}+j\omega_L)x_l} dx_l$$

Performing the integration we obtain

$$\phi_{X_l^2}(j\omega_1) = \frac{1}{\sqrt{2\sigma_{x^2}(\frac{1}{2\sigma_{x^2}}+j\omega_L)}}$$

Since Xls are independent their joint CF is the product of individual CFs, hence

$$\phi_{X_1^2 \dots\dots X_l^2}(j\omega_1, j\omega_1, \dots ., j\omega_L) = \frac{1}{(2\sigma_{x^2})^{L/2}} \prod_{i=1}^{L} \frac{1}{\sqrt{(\frac{1}{2\sigma_{x^2}}+j\omega_i)}}$$

Similarly the joint CF of RVs $Y_1^2 \dots \dots Y_l^2$ can be obtained as

$$\phi_{Y_1^2 \ldots\ldots Y_l^2}(j\omega_1, j\omega_1, \ldots., j\omega_L) = \frac{1}{(2\sigma_{y^2})^{L/2}} \prod_{i=1}^{L} \frac{1}{\sqrt{(\frac{1}{2\sigma_{y^2}} + j\omega_i)}}$$

Hence, the joint CF in Equation can be obtained as

$$\phi_{\alpha_1^2 \ldots\ldots \alpha_l^2}(j\omega_1, j\omega_1, \ldots., j\omega_L) = \phi_{X_1^2 \ldots\ldots X_l^2} = \frac{1}{(2\sigma_{x^2}\sigma_{y^2})^{L/2}} \prod_{i=1}^{L} \frac{1}{\sqrt{(\frac{1}{2\sigma_{x^2}} + j\omega_i)(\frac{1}{2\sigma_{y^2}} + j\omega_i)}}$$

Probability Distribution Analysis

Receiver In this analysis correlation between the fading envelopes α_ls (l = 1,2) is assumed. A general expression for the combiner output SNR γ_{MRC} is given in Equation 3.1. It can be expressed for the dual diversity case as

$$\gamma_{MRC} = \frac{E_b}{N_o}(\alpha_1^2 + \alpha_2^2) \qquad 3.1$$

An expression for the PDF of γmrc i.e. fγmrc (γmrc), when α1 and α2 are correlated with correlation coefficient ρ can be obtained using the complex Gaussian model of Hoyt RV in [13]. Using the PDF fγmrc (γmrc), performance measures such as average output SNR, outage probability and ABER for binary, coherent and non-coherent modulations are derived. PDF of Combiner Output Signal-to-Noise Ratio From Equation 3.1, it can be observed that an expression for the PDF of γmrc can be obtained from the PDF of the RV $\alpha_1^2 + \alpha_2^2$. Using the complex Gaussian model for Hoyt distribution , an expression for the joint CF of RVs $\alpha_1^2$and α_2^2 is reproduced below.

$$\emptyset_{\alpha_1^2,\alpha_2^2}(jw1, jw2)$$
$$= \frac{1}{(1-\rho^2)(2\sigma_x\sigma_y)^2} \sum_{k=0}^{\infty} \sum_{t=0}^{\infty} \frac{(2k-1)!!\,(2t-1)!!}{k!\,t!\left[\left(\frac{1}{2(1-\rho^2)\sigma_x{}^2} + jw1\right)\left(\frac{1}{2(1-\rho^2)\sigma_x{}^2} + jw2\right)\right]^{k+\frac{1}{2}}}$$

$$\times \left[\frac{\rho}{\sqrt{8}\sigma_x{}^2(1-\rho^2)}\right]^{2(k+t)} \frac{1}{\left[\left(\frac{1}{2(1-\rho^2)\sigma_x{}^2} + jw1\right)\left(\frac{1}{2(1-\rho^2)\sigma_y{}^2} + jw1\right)\right]^{t+\frac{1}{2}}} \qquad 3.2$$

An expression for the PDF of $\alpha^2 = \alpha_1^2 + \alpha_2^2$ can be obtained by substituting ω1 = ω2 = ω in Equation 3.2 and subsequently taking the inverse Fourier transform to the resulting expression. This can be given as

$$f_{\alpha^2}(\alpha^2) = \frac{1}{8\pi(1-\rho^2)(\sigma_x\sigma_y)^2}\sum_{k=0}^{\infty}\sum_{t=0}^{\infty}\frac{(2k-1)!!\,(2t-1)!!}{k!\,t!}$$

$$\times\left[\frac{\rho}{\sqrt{8}\sigma_x{}^2(1-\rho^2)}\right]^{2(k+t)}\frac{e^{j\omega\alpha}}{\left(\frac{1}{2(1-\rho^2)\sigma_x{}^2}+jw\right)^{2k+1}\left(\frac{1}{2(1-\rho^2)\sigma_y{}^2}+jw\right)^{2t+1}} \qquad 3.3$$

The combiner output SNR can be given as $\gamma_{mrc} = \left(\frac{Eb}{N0}\right)\alpha^2$. Thus, the PDF of γmrc can be obtained by scaling equation corresponding to the multiplying factor *Eb*/*N*0, applying the concept of transformation of RVs. For identical branch average power i.e. Ω1 = Ω2 = Ω (equivalently, $\overline{\gamma_1} = \overline{\gamma_2} = \overline{\gamma_3} \dots\dots.. = \bar{\bar{\gamma}}$), it can be shown that *Eb*/*N*0 = $\bar{\bar{\gamma}}/(1+q^2)$. Substituting this relation, subsequent to the transformation of RV, an expression for *f*γ*mrc*(γ*mrc*) can be obtained as

$$f_{\gamma_{mrc}}(\gamma_{mrc}) = \left(\frac{(1+q^2)}{2q\sqrt{(1-\rho^2)}\bar{\gamma}}\right)^2\sum_{k=0}^{\infty}\sum_{t=0}^{\infty}\frac{(2k-1)!!\,(2t-1)!!}{k!\,t!\,(2(k+t+1))}\times\left[\frac{\rho(1+q^2)}{\sqrt{8}\bar{\gamma}(1-\rho^2)}\right]^{2(k+t)}$$

Outage Probability

Outage probability is an important performance measure of any communication receiver. For the output SNR, it is defined as the probability that the output SNR γ, falls below a certain threshold value γ*th*. Mathematically, it can be given as

$$P_{out}(\gamma_{th}) = \int_o^{\gamma_{th}} f_\gamma(\gamma)d\gamma$$

Putting *f*γ*mrc*(γ*mrc*) from previous equation into this equation, an expression for the outage probability for correlated dual-MRC receiver can be expressed as

$$P_{out}(\gamma_{th}) = (\frac{(1+q^2)}{2q\sqrt{(1-\rho^2)}\bar{\gamma}})^2 \sum_{k=0}^{\infty}\sum_{t=0}^{\infty} \frac{(2k-1)!!\,(2t-1)!!}{k!\,t!\,(2(k+t+1))} \times [\frac{\rho(1+q^2)}{\sqrt{8}\bar{\gamma}(1-\rho^2)}]^{2(k+t)}$$

$$\times \int_o^{\gamma_{th}} e^{-\frac{(1+q^2)}{2q\sqrt{(1-\rho^2)}q^2}\gamma_{mrc}} {\gamma_{mrc}}^{2k+2t+1} F_1\{2k$$

$$+1; 2(k+t+1); \frac{1-q^4}{2q^2\overline{\gamma(1-\rho^2)}}\gamma_{mrc}\} d\gamma_{mrc}$$

where γth is the threshold value of the combiner output SNR. The integral in Equation 3.45 cannot be solved in the given form. By expressing the hypergeometric function in infinite series, above equation can rewritten as

$$P_{out}(\gamma_{th}) = (\frac{(1+q^2)}{2q\sqrt{(1-\rho^2)}\bar{\gamma}})^2 \sum_{k=0}^{\infty}\sum_{t=0}^{\infty} \frac{(2k-1)!!\,(2t-1)!!}{k!\,t!\,(2(k+t+1))} \times [\frac{\rho(1+q^2)}{\sqrt{8}\bar{\gamma}(1-\rho^2)}]^{2(k+t)}$$

$$\times \int_o^{\gamma_{th}} {\gamma_{mrc}}^{2k+2t+r+1} e^{-\frac{1+q^2}{2q^2\overline{\gamma(1-\rho^2)}}\gamma_{mrc}} \} d\gamma_{mrc}$$

Chapter 4

Results & Discussion

We have earlier noticed that nakagami-q channel or hoyt fading channel is the mathematical formulation of fading in satellite link or other fading which is more similar to actual signal losses. In previous chapter we have described mathematically the hoyt fading channel and its derivation for outage probability for correlated hoyt fading channels. Results have been analysed by outage probability and bit error rate. We have observed the performance of hoyt fading channel considering M-ary modulation and MRC.

MATLAB R2013a has been used as a simulation tool as it provides a wide range of designed mathematical functions which proved to be useful in calculation of channel response. For example the complex calculation of outage probability for MRC is made easier by MATLAB's hypergeometric function, zeroth order Bessel function and gamma function.

Case I- M-ary Modulation in hoyt fading channel

We have tested the performance of nakagami-q channel for 16-PSK modulation. The input data for a short interval is shown in figure 4.1. The constellation diagram for it is shown in figure 4.2.

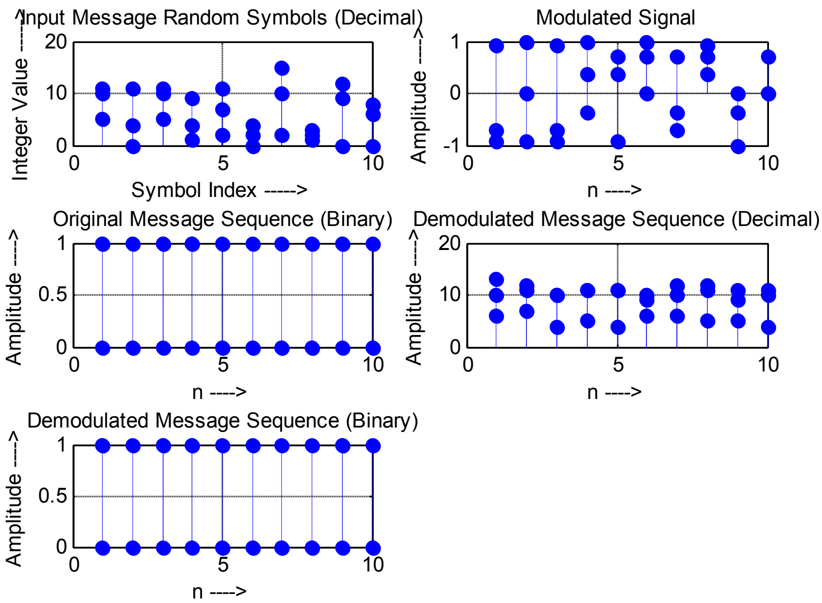

Figure 4.1: 16-PSk modulated input symbol

Constellation diagram provides a graphical representation of the complex envelope of each possible Symbol state. The x- axis of the constellation diagram represents the in-phase component of the complex envelope and the y-axis represents the quadrature component of the complex envelope. The distance between the signals on the constellation diagram relates to how different the modulation waveform are, and how well a receiver can differentiate between all possible symbols when random noise is present.

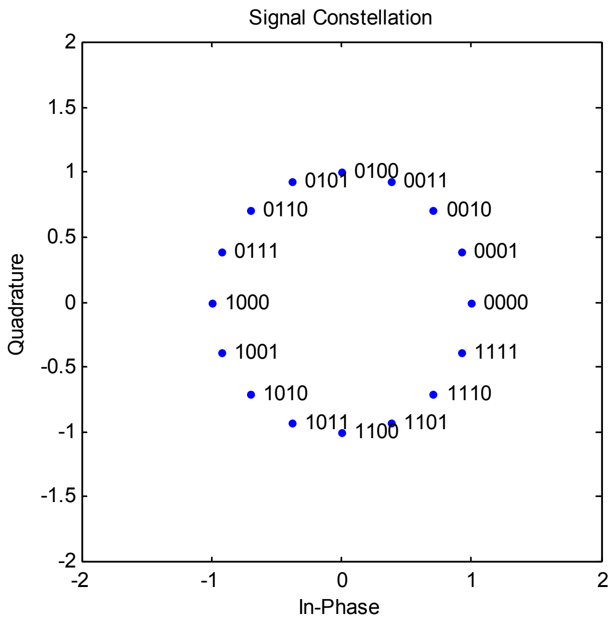

Figure 4.2: constellation diagram of 16-ary PSK modulation

In teh previous chapter the channel response of hoyt fading channel depends upon the hoyt fading parameter. Variation in this value results in change in pdf of channel. Fading parameter (q) is the ratio of unequal variances σ_x and σ_y. A channel response for hoyt channel is shown in figure 4.3. As per central limit theorem if there is sufficiently much scatter, the channel impulse response will be well-modelled as a Gaussian process irrespective of the distribution of the individual components. If there is no dominant component to the scatter, then such a process will have zero mean and phase evenly distributed between 0 and 2π radians. The envelope of the channel response will therefore be Hoyt distributed. In this case for q=0.2 is more similar to Gaussian distribution. The response curve is not ideal which is in case when random variable alpha is 1. We have tested this on different value of alpha which are:

RV alpha	0.0539909665336576	0.247921068062695	0.342198280312217

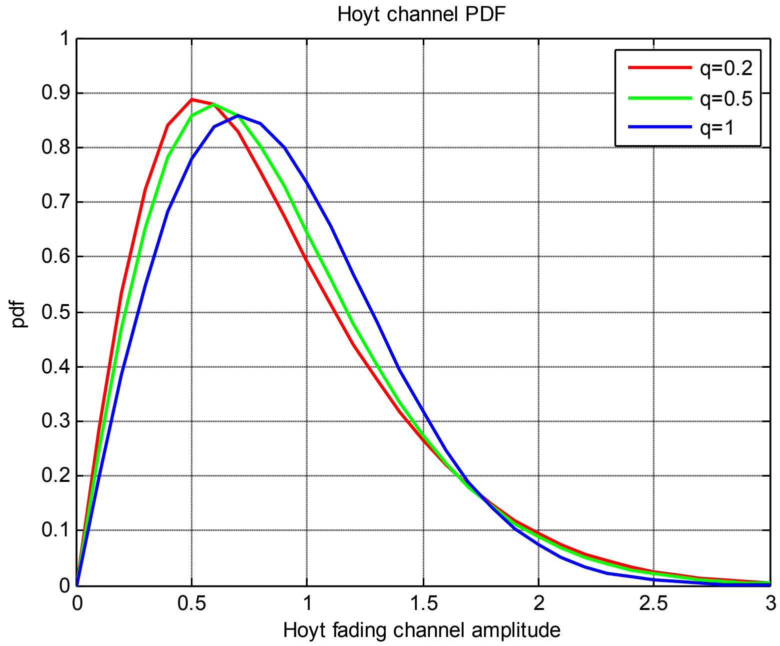

Figure 4.3: channel response of nakagami –q channel

The outage probability curve for 16- ary PSK modulation is shown in figure 4.4. the outage occurs if signal drops below the noise power level. From the figure it is clear that with variation of correlation coefficient ρ, higher values provides less outage probability which means less loss of signal whereas for it is highest for combination of fading coefficient value 1 and correlation coeff =0. From this simulation curve 16- ary PSK modulation it is proved that if fading coeff (q) has range in between 0.4-0.5 and correlation coefficient ρ is 1 then outage in signal will be least. A bit error rate curve for this case is shown in figure 4.5. it must be kept in consideration here that the M-ary simulation has been checked for single transmitter and receiver antenna. The bit error rate curve in 4.5 shows that minimum value is for q-0.5, which is in accordance with outage probability. To validate the simulation results we have tested the M-ary results for 4 and 32 PSK as shown in table 4.1. These simulation curves of outage probability also proves that for q=1 and $\rho = 0$, outage probability is highest in hoyt fading channel. Here $\rho = 0$ represents the un-correlation case as it is correlation coefficient. So in other words for uncorrelated case the hoyt fading channel performs least.

Case II: MRC monte carlo simulation

The next case considered is MRC scheme with monte carlo simulation. In this case we have considered 2 receivers with BPSK modulation. Results have been shown in figure 4.6 and 1.7 for outage probability and bit error rate. These are checked for different values of L, q and ρ. for now only 2 receivers case is being analysed, but the script developed is dynamic and can be used for more number of receivers.

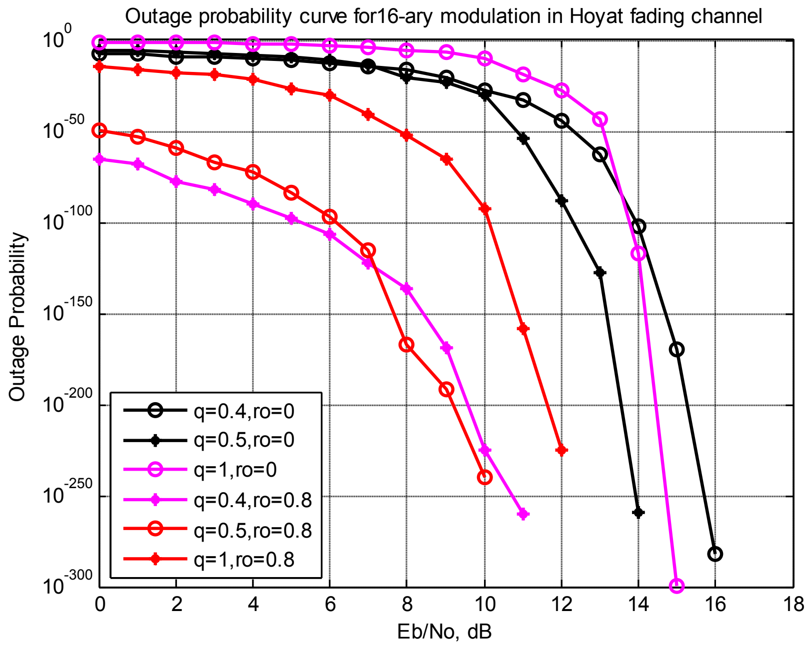

Figure 4.4: outage probability curve for 16-ary simulation of Hoyt fading channel

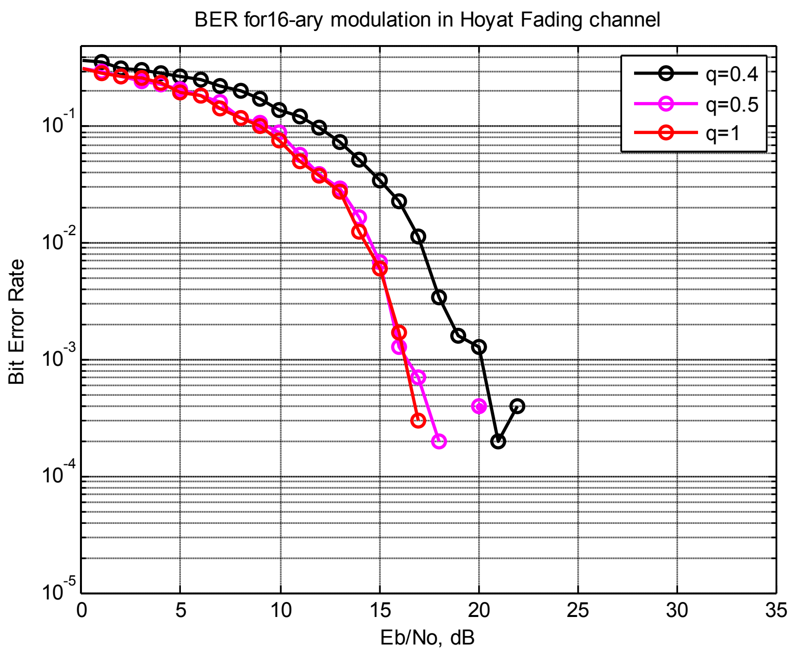

Figure 4.5: BER curve for 16-ary simulation of Hoyt fading channel

Table 4.1: outage probability curve for 4-ary and 32-ary PSK

4-ary	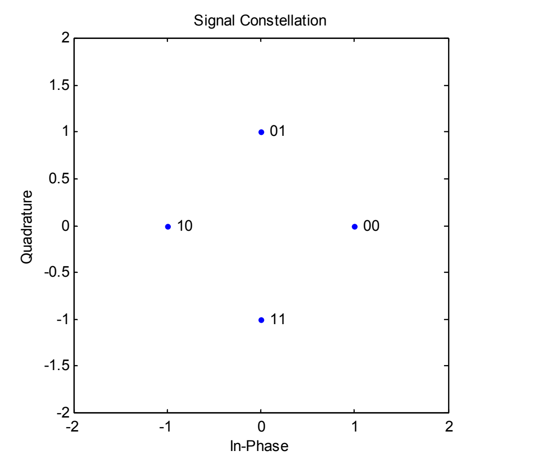	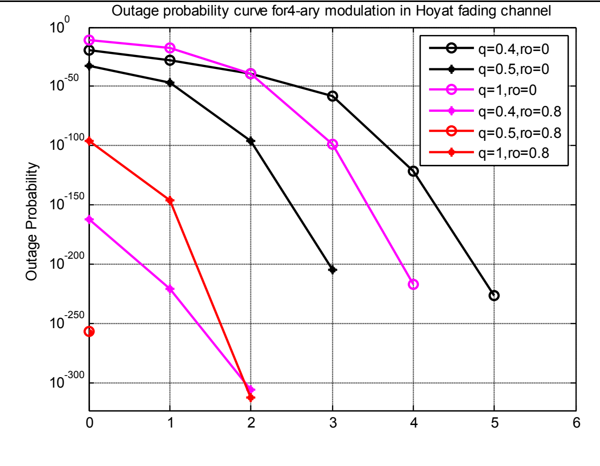
32-ary	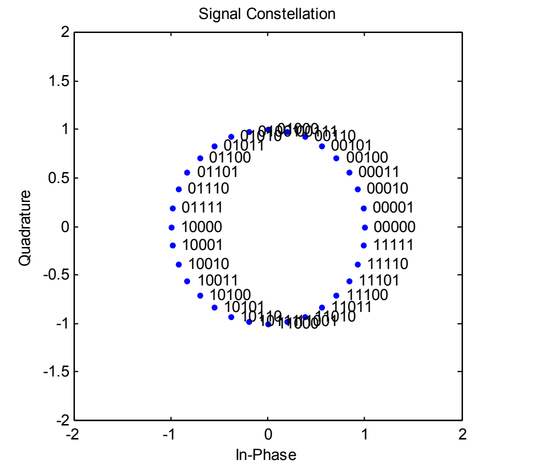	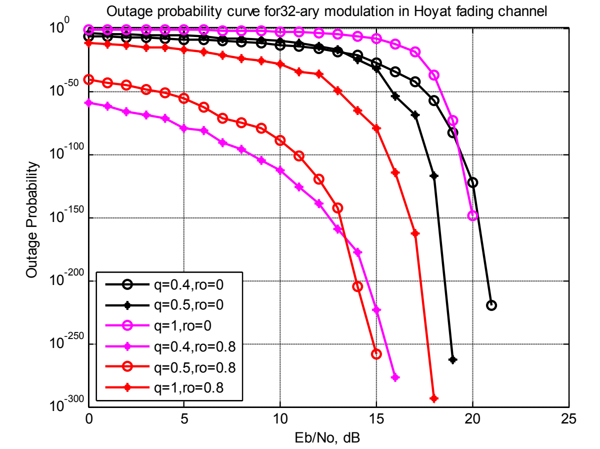

The effect of branch correlation on the outage can be observed by comparing the outage values for ρ =0.8 against the values for ρ =0 (uncorrelated case). Clearly, with the increase in ρ the receiver suffers more outage, for a fixed value of q and L. Again as expected, increase in input branches reduces the probability of outage. The least outage probability is observed at q=0.5, $\rho = 0.8$ and L=2 & maximum outage probability is at q=0.4, $\rho = 0$ and L=1. Similar is the case with BER, for q=0.4 and L=1, it is highest and q=1 and L=2, it is lowest as shown in figure 4.7. So increasing the number of receivers lower the effect of fading in hoyt channel which fulfil the MRC purpose since MRC is used to reduce the noise effect in transmitted signal.

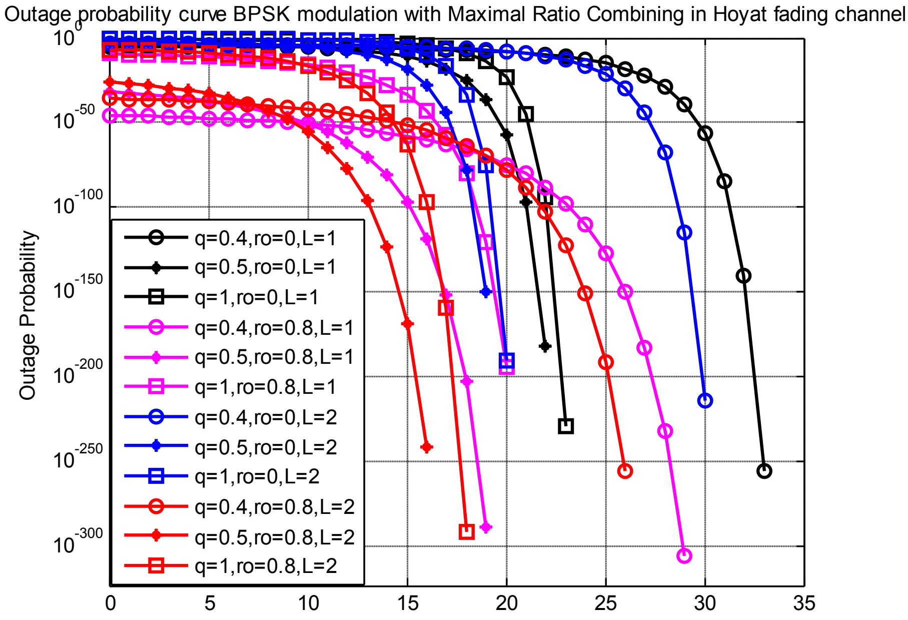

Figure 4.6: outage probability curve for MRC in hoyt fading channel

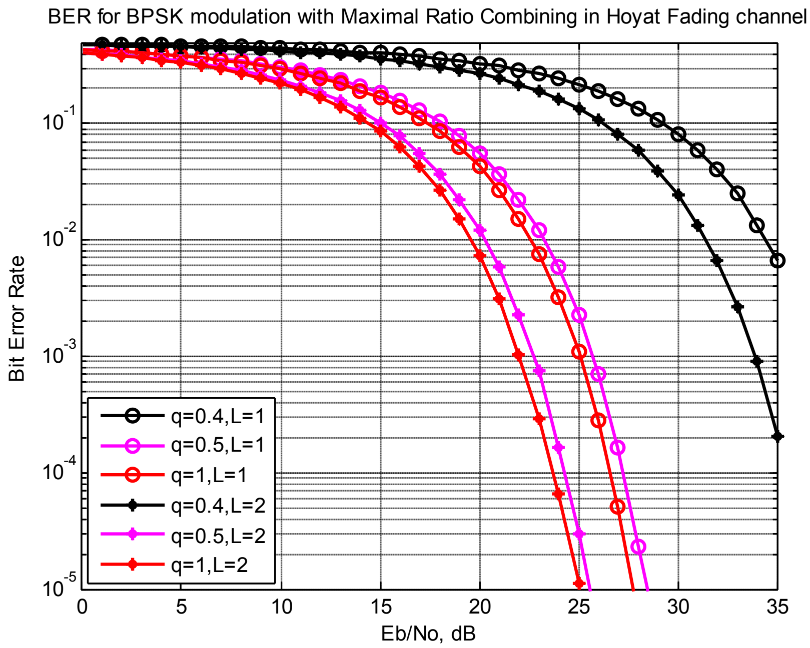

Figure 4.7: BER for MRC in hoyt fading channel

Chapter 5

Conclusion & Future Scope

5.1 Conclusion

Hoyt fading channel is more realistic satellite link channel. In this work, Performance of M-ary modulation scheme and MRC diversity receivers are analyzed over Hoyt fading channels. Focusing on the analytical approach, mathematical expressions for various performance measures such as outage probability and BER of diversity receivers have been obtained. The PDF based analytical approach has been preferred in all analyses for these performance measures, wherever possible. It is stressed to analyze diversity receivers with arbitrary order of diversity with correlated fading channels since these cases are encountered frequently in the field deployment of diversity receivers. Results are compared with various correlation coefficients value of hoyt fading channel and different number of receiver antennas and different set of fading coefficients. It has been observed that in case of M-ary simulation with M=16, fading coeff (q) has range in between 0.4-0.5 and correlation coefficient ρ is 1for least outage probability. These values are validated by checking on 4-ary and 32-ary simulation too.

In case of MRC scheme, 2 receivers are compared for different values of q and ρ. it is observed that with increase in number of antennas, outage probability and BER decreases. The least outage probability is observed at q=0.5, $\rho = 0.8$ and L=2 & maximum outage probability is at q=0.4, $\rho = 0$ and L=1. These results are successfully simulated using MATLAB's communication toolbox.

5.2 Future Work

A few research problems that can be taken up for analysis are enumerated below:

- Performance of L-MRC receivers over correlated Hoyt fading channels with arbitrary fading parameter
- Performance of L -EGC, SC receivers over correlated Hoyt fading channels
- Performance of L -EGC, SC receivers over correlated $\eta - \mu$ fading channels
- Performance of diversity receivers over correlated $\kappa - \mu$ fading channel

References

[1]. Rupaban Subadar and P. R. Sahu," Performance of L-MRC Receiver over Equally Correlated Hoyt Fading Channels", IETE JOURNAL OF RESEARCH, VOL 57, ISSUE 3, MAY-JUN 2011

[2]. Vladeta Milentijević1, Dragan Denić1, Mihajlo Stefanović1,Stefan R. Panić2, Dragan Radenković," Relative Measurement Error Analysis in the Process of the Nakagami-*m* Fading Parameter Estimation", SERBIAN JOURNAL OF ELECTRICAL ENGINEERING Vol. 8, No. 3, November 2011, 341-349

[3]. Suvarna P. Jadhav, Vaibhav S. Hendre," Performance of Maximum ratio combining (MRC) MIMO Systems for Rayleigh Fading Channel", International Journal of Scientific and Research Publications, Volume 3, Issue 2, February 2013

[4]. D.B. Smith and T.D. Abhayapala," Maximal ratio combining performance analysis in practical Rayleigh fading channels", IEE Proc.-Commun., Vol. 153, No. 5, October 2006

[5]. R. Subadar and P. R. Sahu, "Performance of L-MRC receiver over independent Hoyt fading channels," *Communications (NCC), 2010 National Conference on*, Chennai, 2010, pp. 1-5.

[6]. G. K. Karagiannidis, N. C. Sagias and D. A. Zogas, "Error analysis of M-QAM with equal-gain diversity over generalised fading channels," in *IEE Proceedings - Communications*, vol. 152, no. 1, pp. 69-74, 24 Feb. 2005.

[7]. V. G. Venkatesan1, S. Karthik2, P. Agilan," Performance Comparison of L-MRC Receivers over Nakagami-M Fading and Hoyt Fading Channels", International Journal of Science and Research (IJSR), Volume 2 Issue 3, March 2013.

[8]. In-Ho Lee," SER Performance of Enhanced Spatial Multiplexing Codes with ZF / MRC Receiver in Time-Varying Rayleigh Fading Channels", The Scientific World Journal Volume 2014.

[9]. Wamberto J. L. Queiroz, Francisco Madeiro, Waslon Terllizzie A. Lopes, Member, IEEE, and Marcelo S. Alencar, Senior-Member, IEEE," Error Probability of Multichannel Reception with θ-QAM Scheme Under Correlated Nakagami-m Fading, JOURNAL OF COMMUNICATIONS AND INFORMATION SYSTEMS, VOL. 29, NO. 1, MAY 2014"

[10]. R.Deepa, Dr.K.Baskaran, Pratheek Unnikrishnan, Aswath Kumar," Study Of Spatial Diversity Schemes In Multiple Antenna Systems", Journal of Theoretical and Applied Information Technology, 2009

[11]. A K M Arifuzzman, Md. Anwar Hossain, Nadia Nowshin, Mohammed Tarique," A COMPARATIVE PERFORMANCE ANALYSIS OF MRC DIVERSITY RECEIVERS IN OFDM SYSTEM" International Journal of Distributed and Parallel Systems (IJDPS) Vol.2, No.4, July 2011.

[12]. Vivek K. Dwivedi, Pradeep Kumar, and G. Singh," Performance Analysis of OFDM Communication System over Correlated Nakagami-*m* Fading Channel", PIERS Proceedings, Beijing, China, March 23–27, 2009.

[13]. Surbhi Sharma , Palvinder Singh," Analysis of MRC and OC with OFDM In Terms Of BER Using Different Modulation Techniques over Rayleigh Channel", International Journal of Advanced Research in Electrical, Electronics and Instrumentation Engineering *(An ISO 3297: 2007 Certified Organization)* Vol. 3, Issue 6, June 2014

[14]. Satyendra Chadokar, Pravin Barmashe," Performance Evaluation of Equalizers and Different Diversity Techniques using OFDM", International Journal of Computer Technology and Electronics Engineering (IJCTEE), Volume 1, Issue 3,2013

[15]. Marco Krondorf, Gerhard Fettweis," OFDM Link Performance Analysis under Various Receiver Impairments", EURASIP Journal on Wireless Communications and Networking, December 2007

[16]. Juan M. Romero-Jerez, Senior Member, IEEE, and F. Javier Lopez-Martinez, Member, IEEE," A New Framework for the Performance Analysis of Wireless Communications under Hoyt (Nakagami- q)", arXiv:1403.0537v3 [cs.IT] 5 May 2015

[17]. D. A. Zogas, G. K. Karagiannidis and S. A. Kotsopoulos, "Equal gain combining over Nakagami-n (rice) and Nakagami-q (Hoyt) generalized fading channels," in *IEEE Transactions on Wireless Communications*, vol. 4, no. 2, pp. 374-379, March 2005.

[18]. Jos´e F. Paris and David Morales-Jim´enez," Outage Probability Analysis for Nakagami-(Hoyt) Fading Channels under Rayleigh Interference", IEEE TRANSACTIONS ON WIRELESS COMMUNICATIONS, VOL. 9, NO. 4, APRIL 2010.

[19]. R. M. Radaydeh and M. M. Matalgah, "Average BER Analysis for M -ary FSK Signals in Nakagami- q (Hoyt) Fading With Noncoherent Diversity Combining," in *IEEE Transactions on Vehicular Technology*, vol. 57, no. 4, pp. 2257-2267, July 2008.

[20]. Li Tang Zhu Hongbo, Analysis and Simulation of Nakagami Fading Channel with MATLAB", Asia- Pacific Conference on Environmental Electromagnetics CEEM 2003 , China.

[21]. Gayarti S. Prabhu and P.Mohana Shankar "simulation of flat fading using MATLAB for classroom instruction" IEEE Transactions on Education Vo1.45. No.1, Feb. 2002.

[22]. Md. Golam Sadeque, Shadhon Chandra Mohonta, Md. Firoj Ali," Modeling and Characterization of Different Types of Fading Channel", International Journal of Science, Engineering and Technology Research (IJSETR), Volume 4, Issue 5, May 2015

[23]. G. Fraidenraich , O. Leveque and J. M. Cioffi, "On the MIMO channel capacity for Nakagami-m channel", *IEEE Trans. Inf. Theory*, vol. 54, no. 8, pp. 3752-3757, 2008

A. O. Yilmaz, "Calculating Outage Probability of Block Fading Channels Based on Moment Generating Functions," in *IEEE Transactions on Communications*, vol. 59, no. 11, pp. 2945-2950, November 2011.

B. Sanjiv Kumar, P. K. Gupta," Performance Analysis of Rayleigh and Rician Fading Channel Models using Matlab Simulation", *I.J. Intelligent Systems and Applications,* 2013, 09, 94-102

Appendix

M-ary modulation

Phase-shift keying (**PSK**) is a digital modulation scheme that conveys data by changing (modulating) the phase of a reference signal (the carrier wave). The modulation is impressed by varying the sine and cosine inputs at a precise time. It is widely used for wireless LANs, RFID and Bluetooth communication.

Any digital modulation scheme uses a finite number of distinct signals to represent digital data. PSK uses a finite number of phases, each assigned a unique pattern of binary digits. Usually, each phase encodes an equal number of bits. Each pattern of bits forms the symbol that is represented by the particular phase. The demodulator, which is designed specifically for the symbol-set used by the modulator, determines the phase of the received signal and maps it back to the symbol it represents, thus recovering the original data. This requires the receiver to be able to compare the phase of the received signal to a reference signal — such a system is termed coherent (and referred to as CPSK).

Alternatively, instead of operating with respect to a constant reference wave, the broadcast can operate with respect to itself. Changes in phase of a single broadcast waveform can be considered the significant items. In this system, the demodulator determines the changes in the phase of the received signal rather than the phase (relative to a reference wave) itself. Since this scheme depends on the difference between successive phases, it is termed **differential phase-shift keying (DPSK)**. DPSK can be significantly simpler to implement than ordinary PSK, since there is no need for the demodulator to have a copy of the reference signal to determine the exact phase of the received signal (it is a non-coherent scheme). In exchange, it produces more erroneous demodulation.

There are three major classes of digital modulation techniques used for transmission of digitally represented data:

- Amplitude-shift keying (ASK)
- Frequency-shift keying (FSK)
- Phase-shift keying (PSK)

All convey data by changing some aspect of a base signal, the carrier wave (usually a sinusoid), in response to a data signal. In the case of PSK, the phase is changed to represent the data signal. There are two fundamental ways of utilizing the phase of a signal in this way:

- By viewing the phase itself as conveying the information, in which case the demodulator must have a reference signal to compare the received signal's phase against; or
- By viewing the *change* in the phase as conveying information — *differential* schemes, some of which do not need a reference carrier (to a certain extent).

A convenient method to represent PSK schemes is on a constellation diagram. This shows the points in the complex plane where, in this context, the real and imaginary axes are termed the in-phase and quadrature axes respectively due to their 90° separation. Such a representation on perpendicular axes lends itself to straightforward implementation. The amplitude of each point along the in-phase axis is used to modulate a cosine (or sine) wave and the amplitude along the quadrature axis to modulate a sine (or cosine) wave. By convention, in-phase modulates cosine and quadrature modulates sine.

In PSK, the constellation points chosen are usually positioned with uniform angular spacing around a circle. This gives maximum phase-separation between adjacent points and thus the best immunity to corruption. They are positioned on a circle so that they can all be transmitted with the same energy. In this way, the moduli of the complex numbers they represent will be the same and thus so will the amplitudes needed for the cosine and sine waves. Two common examples are "binary phase-shift keying" (BPSK) which uses two phases, and "quadrature phase-shift keying" (QPSK) which uses four phases, although any number of phases may be used. Since the data to be conveyed are usually binary, the PSK scheme is usually designed with the number of constellation points being a power of 2.

Definitions

For determining error-rates mathematically, some definitions will be needed:

- E_b = Energy-per-bit
- E_s = Energy-per-symbol = nE_b with *n* bits per symbol

- T_b = Bit duration
- T_s = Symbol duration
- $N_0/2$ = Noise power spectral density (W/Hz)
- P_b = Probability of *bit-error*
- P_s = Probability of symbol-error

$Q(x)$ will give the probability that a single sample taken from a random process with zero-mean and unit-variance Gaussian probability density function will be greater or equal to x. It is a scaled form of the complementary Gaussian error function:

$$Q(x) = \frac{1}{\sqrt{2\pi}} \int_x^{\infty} e^{-t^2/2} dt = \frac{1}{2} \operatorname{erfc}\left(\frac{x}{\sqrt{2}}\right), \; x \geq 0.$$

The error-rates quoted here are those in additive white Gaussian noise (AWGN). These error rates are lower than those computed in fading channels, hence, are a good theoretical benchmark to compare with.

Binary phase-shift keying (BPSK)

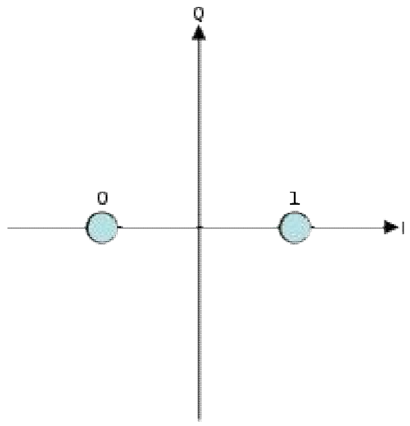

Constellation diagram example for BPSK.

BPSK (also sometimes called PRK, phase reversal keying, or 2PSK) is the simplest form of phase shift keying (PSK). It uses two phases which are separated by 180° and so can also be termed 2-PSK. It does not particularly matter exactly where the constellation points are positioned, and in this figure they are shown on the real axis, at 0° and 180°. This modulation is the most robust of all the PSKs since it takes the highest level of noise or distortion to make the demodulator reach an incorrect decision. It is, however, only able to modulate at 1 bit/symbol (as seen in the figure) and so is unsuitable for high data-rate applications.

In the presence of an arbitrary phase-shift introduced by the communications channel, the demodulator is unable to tell which constellation point is which. As a result, the data is often differentially encoded prior to modulation.

BPSK is functionally equivalent to 2-QAM modulation.

Implementation

The general form for BPSK follows the equation:

$$s_n(t) = \sqrt{\frac{2E_b}{T_b}} \cos(2\pi f_c t + \pi(1 - n)), n = 0, 1.$$

This yields two phases, 0 and π. In the specific form, binary data is often conveyed with the following signals:

$$s_0(t) = \sqrt{\frac{2E_b}{T_b}} \cos(2\pi f_c t + \pi) = -\sqrt{\frac{2E_b}{T_b}} \cos(2\pi f_c t)$$ for binary "0"

$$s_1(t) = \sqrt{\frac{2E_b}{T_b}} \cos(2\pi f_c t)$$ for binary "1"

where f_c is the frequency of the carrier-wave.

Hence, the signal-space can be represented by the single basis function

$$\phi(t) = \sqrt{\frac{2}{T_b}} \cos(2\pi f_c t)$$

where 1 is represented by $\sqrt{E_b}\phi(t)$ and 0 is represented by $-\sqrt{E_b}\phi(t)$. This assignment is, of course, arbitrary.

This use of this basis function is shown at the end of the next section in a signal timing diagram. The topmost signal is a BPSK-modulated cosine wave that the BPSK modulator would produce. The bit-stream that causes this output is shown above the signal (the other parts of this figure are relevant only to QPSK).

Bit error rate

The bit error rate (BER) of BPSK in AWGN can be calculated as:

$$P_b = Q\left(\sqrt{\frac{2E_b}{N_0}}\right) \text{ or } P_e = \frac{1}{2}\operatorname{erfc}\left(\sqrt{\frac{E_b}{N_0}}\right)$$

Since there is only one bit per symbol, this is also the symbol error rate.

Quadrature phase-shift keying (QPSK)

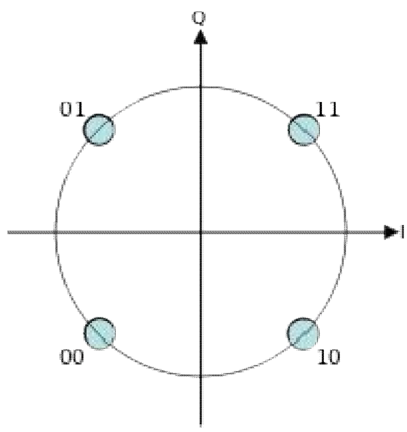

Constellation diagram for QPSK with Gray coding. Each adjacent symbol only differs by one bit.

Sometimes this is known as *quadriphase PSK*, 4-PSK, or 4-QAM. (Although the root concepts of QPSK and 4-QAM are different, the resulting modulated radio waves are exactly the same.) QPSK uses four points on the constellation diagram, equispaced around a circle. With four phases, QPSK can encode two bits per symbol, shown in the diagram with Gray coding to minimize the bit error rate (BER) — sometimes misperceived as twice the BER of BPSK.

The mathematical analysis shows that QPSK can be used either to double the data rate compared with a BPSK system while maintaining the *same* bandwidth of the signal, or to *maintain the data-rate of BPSK* but halving the bandwidth needed. In this latter case, the BER of QPSK is *exactly the same* as the BER of BPSK - and deciding differently is a common confusion when considering or describing QPSK. The transmitted carrier can undergo numbers of phase changes.

Given that radio communication channels are allocated by agencies such as the Federal Communication Commission giving a prescribed (maximum) bandwidth, the advantage of QPSK over BPSK becomes evident: QPSK transmits twice the data rate in a given bandwidth compared to BPSK - at the same BER. The engineering penalty that is paid is that QPSK transmitters and receivers are more complicated than the ones for BPSK. However, with modern electronics technology, the penalty in cost is very moderate.

As with BPSK, there are phase ambiguity problems at the receiving end, and differentially encoded QPSK is often used in practice.

Implementation

The implementation of QPSK is more general than that of BPSK and also indicates the implementation of higher-order PSK. Writing the symbols in the constellation diagram in terms of the sine and cosine waves used to transmit them:

$$s_n(t) = \sqrt{\frac{2E_s}{T_s}} \cos\left(2\pi f_c t + (2n-1)\frac{\pi}{4}\right), \quad n = 1,2,3,4.$$

This yields the four phases $\pi/4$, $3\pi/4$, $5\pi/4$ and $7\pi/4$ as needed.

This results in a two-dimensional signal space with unit basis functions

$$\phi_1(t) = \sqrt{\frac{2}{T_s}} \cos(2\pi f_c t)$$

$$\phi_2(t) = \sqrt{\frac{2}{T_s}} \sin(2\pi f_c t)$$

The first basis function is used as the in-phase component of the signal and the second as the quadrature component of the signal.

Hence, the signal constellation consists of the signal-space 4 points

$$\left(\pm\sqrt{E_s/2}, \pm\sqrt{E_s/2}\right).$$

The factors of 1/2 indicate that the total power is split equally between the two carriers.

Comparing these basis functions with that for BPSK shows clearly how QPSK can be viewed as two independent BPSK signals. Note that the signal-space points for BPSK do not need to split the symbol (bit) energy over the two carriers in the scheme shown in the BPSK constellation diagram.

QPSK systems can be implemented in a number of ways. An illustration of the major components of the transmitter and receiver structure are shown below.

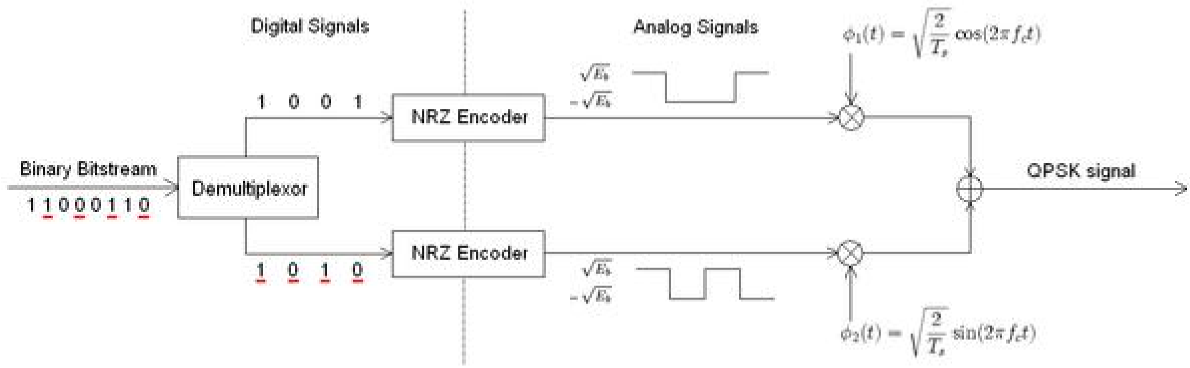

Conceptual transmitter structure for QPSK. The binary data stream is split into the in-phase and quadrature-phase components. These are then separately modulated onto two orthogonal basis functions. In this implementation, two sinusoids are used. Afterwards, the two signals are superimposed, and the resulting signal is the QPSK signal. Note the use of polar non-return-to-zero encoding. These encoders can be placed before for binary data source, but have been placed after to illustrate the conceptual difference between digital and analog signals involved with digital modulation.

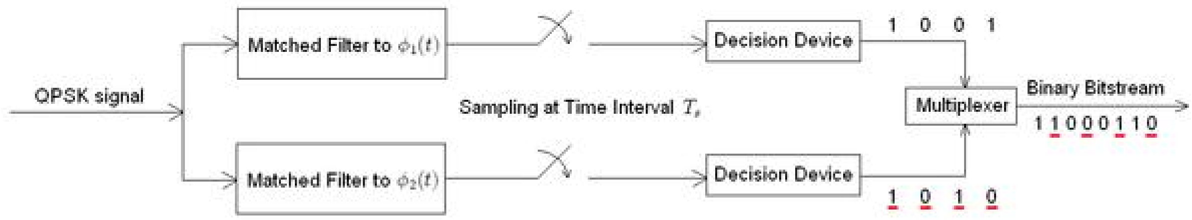

Receiver structure for QPSK. The matched filters can be replaced with correlators. Each detection device uses a reference threshold value to determine whether a 1 or 0 is detected.

Bit error rate

Although QPSK can be viewed as a quaternary modulation, it is easier to see it as two independently modulated quadrature carriers. With this interpretation, the even (or odd) bits are used to modulate the in-phase component of the carrier, while the odd (or even) bits are used to modulate the quadrature-phase component of the carrier. BPSK is used on both carriers and they can be independently demodulated.

As a result, the probability of bit-error for QPSK is the same as for BPSK:

$$P_b = Q\left(\sqrt{\frac{2E_b}{N_0}}\right).$$

However, in order to achieve the same bit-error probability as BPSK, QPSK uses twice the power (since two bits are transmitted simultaneously).

The symbol error rate is given by:

$$P_s = 1 - (1 - P_b)^2$$

$$= 2Q\left(\sqrt{\frac{E_s}{N_0}}\right) - \left[Q\left(\sqrt{\frac{E_s}{N_0}}\right)\right]^2.$$

If the signal-to-noise ratio is high (as is necessary for practical QPSK systems) the probability of symbol error may be approximated:

$$P_s \approx 2Q\left(\sqrt{\frac{E_s}{N_0}}\right)$$

The modulated signal is shown below for a short segment of a random binary data-stream. The two carrier waves are a cosine wave and a sine wave, as indicated by the signal-space analysis above. Here, the odd-numbered bits have been assigned to the in-phase component and the even-numbered bits to the quadrature component (taking the first bit as number 1). The total signal — the sum of the two components — is shown at the bottom. Jumps in phase can be seen as the PSK changes the phase on each component at the start of each bit-period. The topmost waveform alone matches the description given for BPSK above.